Applied Biosafety

www.absa.org

Volume 19, Number 4, 2014

Journal of the American Biological Safety Association

The Effects of Patient Movement on Particles Dispersed by Coughing in an Indoor Environment

Yanzheng (Don) Guan*, Alamelu Ramesh, and Farhad Memarzadeh

National Institutes of Health, Bethesda, Maryland

Abstract

This study investigates the influence of a moving patient on the transport characteristics of coughing particles by dynamic meshing and the Lagrangian particle tracking method. Through simulation, particle movement during the initial coughing, patient movement, and stationary flow phases was examined. Two different particle sizes (5 µm and 10 µm) were used and yielded small differences in the initial airflow after coughing. During the patient-moving phase, the temporal particle distribution in the upper, breathing, lower, and near-floor zones were simulated. The amplified air-velocity field induced by the moving patient enhanced the particle entrainment, thus increasing the risk of contamination (defined as particle system entropy) in the whole room. Both temporal and final particle distribution during the stationary flow phase were studied. Walking speed affected the particle distribution in the traveling direction, but not in the vertical or lateral directions at the end of the simulation. Turbulence dispersion played a critical role in the spread of the particles through the coughing and patient-moving phases.

Keywords

Computational Fluid Dynamics, Coughing, Dynamic Meshing, Particle Tracking, Infectious Disease Transmission, and Ventilation

Introduction

Exhaled particles play a key role in analyzing the pathway of an airborne microorganism. Extensive studies have been conducted on the generation, transport, and removal of the expiratory particles in hospital wards and transportation vehicles. However, few investigations on the effects of human movements (such as a walking patient, caretaker, or visitor) on micron-scale particle dispersion over a relatively long duration have been conducted. This study investigates the dynamic interactions between the airflow generated by patient movement and the particles discharged by coughing.

Literature Review

Body Movement in Computational Fluid Dynamics (CFD) Simulations

Because the direct CFD simulation of a moving human body via dynamic meshing (i.e., to simulate flows where the geometry changes with time, the computational grid changes dynamically during the CFD simulation) and particle tracking at each time step is computationally intensive for a large space, indirect approaches, such as a distributed momentum source (Hathway, 2008; Zhai et al., 2002), volume flux (Memarzadeh, 2010), a turbulent kinetic energy source (Brohus et al., 2006), and a "wind tunnel" approach (Ge et al., 2013), were developed to approximate body displacement. The "direct" simulation of human walking works by updating the mesh at each time interval. Lin and Zhao (2012) simulated a moving human body (speed 0-1.5 m/s) and its effects on indoor airflow and contaminants. They found that the air velocity in a room with a ventilation rate of 10 air changes per hour (ACH) could quickly return to the steady-state condition. However, if the air change rate was reduced to 3-6 ACH, or the displacement ventilation (i.e., the room air distribution strategy where conditioned air is supplied at floor level and extracted above the occupied zone, usually at ceiling height) was selected, the recovery time was extended. When the movement took place only once, the environment could return to its steady-state condition in 15-60 seconds after the person stopped walking. However, the indoor environment would be significantly changed by ongoing movement. The Eulerian approach (i.e., a way to study fluid motion that focuses on specific locations through which the fluid flows as time passes. This can be visualized by sitting on the bank of a river and watching as the water passes the fixed location) was utilized throughout Mazumdar's studies (Mazumdar, 2008; Mazumdar & Chen, 2007; Mazumdar et al., 2010) of human movement in an inpatient ward (at 1 m/s for 120 seconds) and an aircraft cabin (at 1.75 m/s and 0.61 m/s for 5.2 seconds and 15 seconds, respectively). Their results showed that a moving airplane passenger could carry a contaminant in the wake zone up to 9-10 seating rows from a coughing individual. Three different body geometries—a rectangular block, a cylinder, and a human-like model—were examined. It was found that the cylinder carried the least amount of contaminant along the traveling direction.

Poussou et al. (2010) performed both a CFD study and a particle image velocimetry (PIV) study with a scaled aircraft cabin model in a water tank to validate the CFD model. The PIV results showed a symmetric downwash flow along the vertical centerline of the moving body. The dynamic flow pattern was further disturbed by the flow from the aircraft cabin climate-control system.

Impact of Body Movement Simulations on Particle Distribution

Wang and Chow (2011) evaluated the impact of walking speed on airflow and the number of suspended droplets in an airborne-infection isolation room in a 15-second simulation. Four sizes of particles—0.5 μm, 5 μm, 10 μm, and 20 μm—were simulated. The authors concluded that the faster the walking speed, the longer the wake behind the human body and the fewer the amount of suspended droplets left in the room. Body motion accelerated particle movement and increased the amount of particles escaping through the air outlet. Consequently, the infection risk of the walking person could be reduced.

Choi and Edwards (2008, 2012) investigated the clean room particulate transportation (large eddy simulation with the Eulerian particle tracking approach) induced by human and door motions. A human kinematics model was employed to represent walking activities. A room-room and room-hall configurations were studied and the effects of the human walking pattern, door operation, overpressure level, and vestibule size were examined. The results indicated that a faster walking speed or larger vestibule could reduce contaminant mass transport. The swinging-door motion was the dominant transport mechanism. The human-induced wake transported material over a distance of about 8 meters, which enhanced compartment-to-compartment contaminant transport.

In all of the studies cited above, none of the moving persons cough, so it is not clear how an individual's movement would interact with the particles when the person passes through the "particle cloud" generated by his or her cough.

The Flow Dynamics and Velocity Boundary Conditions of Coughing

Coughing is a complicated multiphase, highly transient velocity during a short period (<0.5 s). The physical and physiological mechanisms of coughing, such as the particle size distribution and vortex dynamics, are still under investigation. Unlike other physical phenomena, the "inner-subject" (within-subject) and "inter-subject" (between-subjects) variability is significantly large: No two people cough alike, and for a given person every cough is a bit (or a lot) different from previous and future coughs.

The transient velocity profiles of airflow from a cough have been investigated by Schlieren imaging (i.e., a flow visualization method used to photograph the flow of fluids of varying density) and PIV technologies. A peak velocity ranging from 6-28 m/s was reported in a number of studies (Chao et al., 2009; Ersahin, 2007; Kwon et al., 2012; Sun & Ji, 2007; Tang et al., 2006; VanSciver et al., 2011; Zhu et al., 2006).

Gupta, Lin, and Chen (2009) conducted an experimental study on the transient flow dynamics of coughing with 12 female and 13 male human subjects. A dynamic exhale airflow curve was derived, which has been specified as the coughing velocity boundary condition in the recent coughing CFD studies by Gupta, Lin, and Chen (2011), Memarzadeh and Xu (2012), and Zhang and Li (2012).

Initial Particle Concentration Generated by Coughing

Only a few recent studies, with a limited number of human subjects, have examined the initial droplet size distribution and concentration generated by coughing. Collection media with subsequent microscopic analyses were detailed in some early studies (Duguid, 1945, Loudon & Roberts, 1967), with the droplet size measured by the collection media mainly in the supermicron range. The air sampling-based optical particle counters, such as the aerodynamic particle sizer (APS) and the scanning mobility particle sizer (SMPS), were used by Fairchild and Stampfer (1987), Papineni and Rosenthal (1997), and Yang et al. (2007). Most of the droplet sizes measured by particle-counter methods are in the submicron range. Optical particle remote-sensing techniques, such as high-speed photography or interferometric Mie imaging (IMI) methods (i.e., an interferometric laser imaging technique which exploits the interference between light reflected from and refracted through individual droplets allowing temporally resolved droplet-size distributions), do not require air sampling, so the measurement plane can be placed very close to the mouth without disturbing the expiratory flow. One of the major limitations of the remote-sensing techniques is the minimum particle-detection size. For example, only droplets larger than 10 μm or 2 μm could be detected by high-speed photography (Jennison, 1942) and by IMI (Chao et al., 2009), respectively. So far, no single technology can detect all exhaled aerosol particles in the full-size range.

Chao et al. (2009), Morawska et al. (2009), and Johnson et al. (2011) conducted extensive research on droplets produced from different respiratory activities by an expiratory droplet investigation system (EDIS). The EDIS consists of a modular HEPA- (high-efficiency particulate air) filtered air-wind tunnel and has been used in combination with a variety of sizing techniques (G. R. Johnson and L. Morawska, personal communication, 2013).

In a study using EDIS with APS (Morawska et al., 2009; particle size range: 0.5-20 μm), typically the droplets dried to equilibrium size by the time the APS measured them. The APS has a reduced sensitivity at the extremes of its particle-size range. The EDIS wind tunnel flow was on for most measurements to filter the background particles.

In a study using EDIS with IMI (Chao et al., 2009; particle size range: >2 μm), the authors' method was effectively instantaneous: Droplets were sized as they passed the measurement point, so typically these particles may still have been evaporating or growing. During the test, the EDIS clean flow was off for most measurements and the EDIS tunnel was open at each end. Three limitations of this technique were: 1) the measurement plane was small (8.9 mm × 6.7 mm) so the exhaled breath may not have been fully captured; 2) the background particle interference and re-entrainment of exhaled breath would affect the results if not eliminated by using the flow of filtered background air;

and 3) the expiratory droplets smaller than the detection limit could not be characterized.

In a study using EDIS with DDA (droplet deposition analysis) (Johnson et al., 2011; particle-size range: >20 µm), the particles were larger and took much longer to undergo evaporation or growth. Again, the EDIS clean flow was off for most measurements. High sensitivity at the low end of the particle-size range was observed. The results from APS and DDA were also integrated to present the full range of the exhaled particle size.

Testing Protocols and Results

APS and IMI, in fact any aerosol measurement technique focusing on the airborne size range, are prone to error when attempting to measure exhaled aerosol due to the entrainment of background aerosol and the re-entrainment of previously emitted breath aerosol. Therefore, removing all background particles from the testing domain except those generated from the human subjects is crucial. The APS result may be more accurate than the IMI result because the EDIS clean airflow was on during the APS test and the particle detection range is wider in the APS system. The DDA results would not be affected by entrainment of previous breath aerosols or of background aerosol, especially for the larger droplets, because the recovered droplets used in the DDA analysis all contained blue food coloring that had been used as a mouth rinse and the particles were traced under a light microscope.

Regarding the testing protocols, the main concern is whether the coughing was representative of a natural cough or not. Is the cough of a healthy person representative of one who is suffering from a serious respiratory infection? The APS, IMI, and DDA results were all subject to this question.

Table 1 gives the particle concentrations from recent coughing studies. The concentrations presented by Yang et al. (2007) were three orders of magnitude larger than those reported by other recent studies (Edwards et al., 2004; Papineni, & Rosenthal, 1997). This large discrepancy might be due to contamination of the sample by the HEPA filter or due to the testing protocols (Morawska et al., 2009). For example, in Yang et al. (2007), when the warm and water-vapor-saturated aerosol from the respiratory tract was transferred to a dry bag at lower room temperature, the supersaturated sample would have moved from the gas phase to the liquid. Consequently, the measured droplets could be much more than that of the aerosol in the respiratory tract. In addition, homogenous nucleation (i.e., nucleation without preferential nucleation sites or surfaces) may have occurred, which significantly increased the number of droplets.

Methodology and CFD Model Setup

A generic hospital room 5 m (L) x 2.5 m (H) x 3 m (W) with a 1.7-m height human-shaped patient (Figure 1) was simulated. The mouth of the patient was 2 cm x 2 cm at a height of 1.5 m, which was the same as the size used

Table 1

Initial coughing particle concentrations from recent studies.

	Morawska et al. (2009)	Chao et al. (2009)	Papineni and Rosenthal (1997)	Yang et al. (2007)	Fairchild and Stampfer (1987)
Coughing particle concentration #/cm^3	0.64	2.4-5.2	0.024-0.22	881-2355	0.6
Number of human subjects	15	11 (3 men and 8 women); 50 coughs per test	5	54 (10-50 years of age)	5 Men

Figure 1

Geometry layout and mesh in the CFD model.

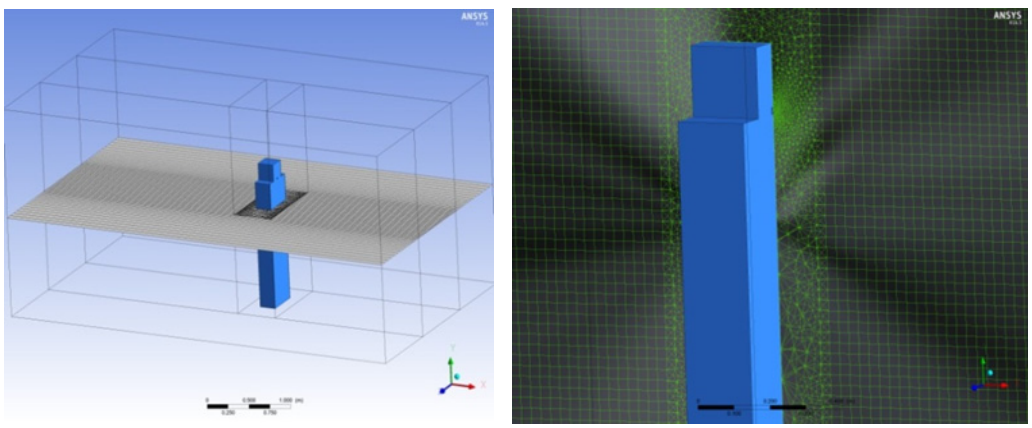

by Gupta, Lin, and Chen (2011). Tetra mesh (0.1-0.5 cm) was used in the near-patient zone, and hexahedral mesh (3 cm) was used in the rest of the space. A total of 1.16 million cells were used.

To save the computational cost, the domain was divided by non-conformal interfaces into one center "moving zone" and two "static zones" on the two sides of the moving zone. Both re-meshing and layering dynamic meshing methods were tested; the layering method was preferred as only local re-meshing was required near the human surfaces at each time step, so the total mesh size and computational time were smaller than "re-meshing" technology (ANSYS, Inc., 2013).

Several scenarios were simulated (Table 2). The patient was initially positioned 0.6 m away from the wall. The patient first walked in a straight line (along +X direction) for 0.09 seconds to initialize the flow, then the patient stopped and coughed once (0.09-0.5 seconds). After coughing, the patient continued to walk for 3.8 seconds until he reached the endpoint close to the opposite wall. The patient could not move more than one-cell distance per time step; thus, the maximum time step was limited to 0.03 seconds. The patient stayed at the endpoint and the simulation continued for 400 seconds. A special simulation without patient movement had also been conducted (Case 4) to compare results with those of a walking patient.

The cough function derived by Gupta et al. (2009) was used for the velocity boundary condition. A Lagrangian-based stochastic particle tracking method was used. Lagrangian specification of the flow field is a way of studying fluid motion where the observer follows an individual fluid parcel as it moves through space and time. This can be visualized as sitting in a boat and drifting down a river. To simplify the simulation and programming, 1 particle/cm^3 was used in this study.

The surface-injection method was used in the CFD model. Because only 38 mesh facets were available from the mouth surface, two particle injections were defined and synchronized to discharge the required particles per time step. Seven hundred eighty-nine particles were injected through a cough based on the cough airflow boundary condition (Gupta et al., 2009).

Two typical walking speeds, 1.0 m/s (2.24 mph) and 0.6 m/s (1.34 mph), and two particle sizes, 5 μm and 10 μm, were simulated. No air-distribution system was modeled in this study, so the behavior of the moving patient and the particle movement could be the focus. A planned future study will investigate the impacts from various mechanical ventilation systems. All walls were modeled as non-trapped walls. A planned future study will investigate the interactions between particles and different wall conditions (escape, reflect, and trap). A RNG k-ε turbulence model was used for all cases as this model generally obtains acceptable accuracy with affordable computation cost for indoor environment-related engineering applications.

Each case experienced three major phases: The initial coughing phase (0.09-0.5 seconds) was characterized as a coughing dynamics-dominated phase; followed by the patient moving phase (0.5-3.8 seconds) in which patient movement and turbulence dispersion were dominant; and finally, the stationary flow phase (3.8-400 seconds) during which the flow stochastic processes dominated.

To examine the transient-particle concentration in the room, the domain was divided into four zones in the direction of height (y coordinate): the upper zone ($1.8 < y < 2.5$ m), the breathing zone ($1.4 < y < 1.8$ m), the lower zone ($0.15 < y < 1.4$ m), and the near-floor zone ($0 < y < 0.15$ m).

Results and Discussion

Initial Coughing Phases (0-0.5 Seconds)

Because of the limitations of current real-time optical flow and particle-measurement technologies (size of the particles, the measurement plane area or image pixel size, etc.), examining the numerical results from the transient coughing process in the initial phase is critical. As shown in Figures 2-5, at the end of a cough (0.48 seconds), the "particle cloud" diameter was approximately 0.58-0.6 m (Figure 3), spreading slightly wider in the y direction due to gravity force (Figures 4 and 5). The different particle sizes (5 μm and 10 μm) yielded little difference as the particle dispersion behaviors in this phase were dominated by the near-field coughing flow. The "young" particles (ID 500-670) had less variation than the "old" particles (ID 1-400). The "newborn" particles (ID 700-789) were still moving so their variation was also high due to turbulence dispersion (Figure 4). Turbulence dispersion (stochastic random walking) plays a critical role in the spread of the particles in the initial coughing phase. Figure 6 displays the particle distribution at the end of coughing (0.48 seconds) with the turbulence dispersion model switched off. Comparing Figure 6 with the two images (time = 0.48 seconds) at the bottom

Table 2

Summary of the cases simulated.

Case #	Particle Size (μm)	Walking Speed (m/s)
1 (base)	10	1.0
2	5	1.0
3	10	0.6
4	10	0
5	5	0

Figure 2

Particle dispersion during the initial coughing phase, colored by the particle residence time.
Case 5: No patient movement. (Fig 2-1, Left) Particle residence time. (Figure 2-2, Right) Particle velocity.

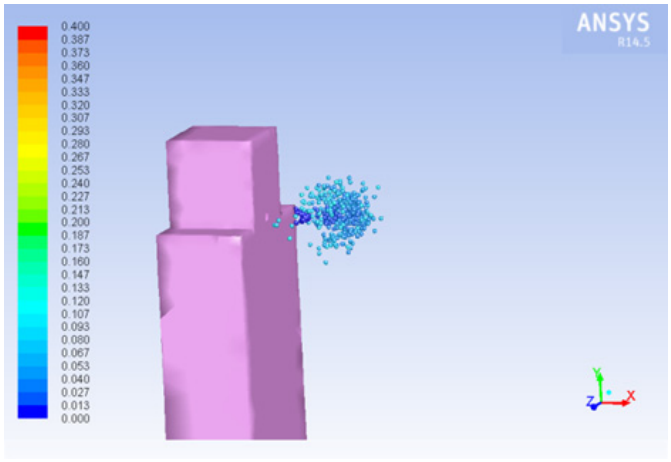

Fig 2-1A Particles colored by residence time (flow t= 0.2 s).

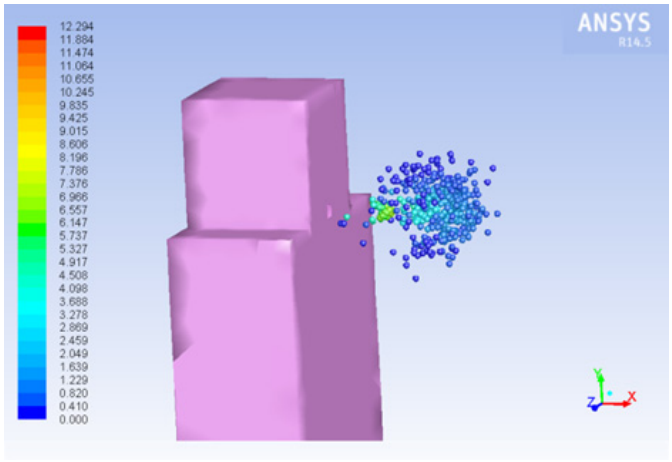

Figure 2-2A Particle velocity (m/s) at flow time = 0.2 sec.

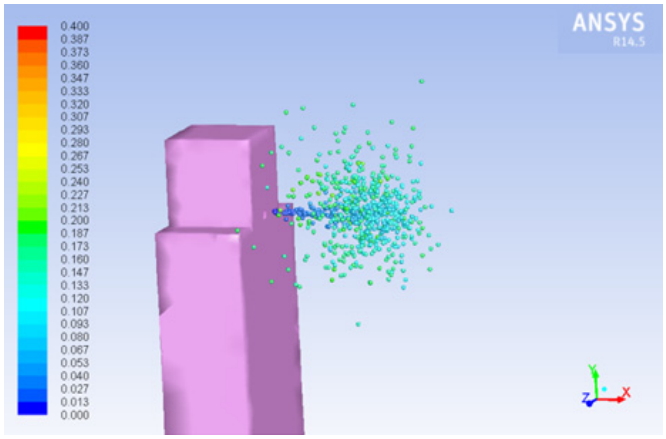

Fig 2-1B Particles colored by residence time (flow t= 0.3 s).

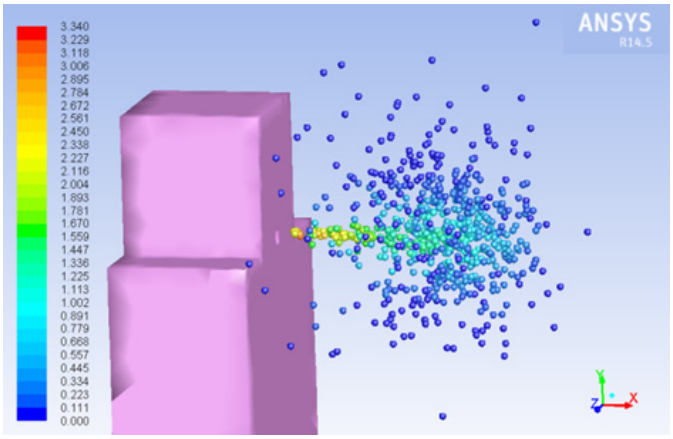

Figure 2-2B Particle velocity (m/s) at flow time = 0.3 s.

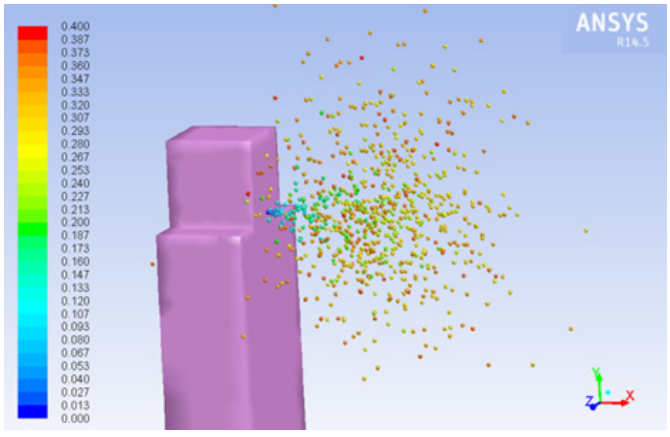

Fig 2-1C Particles colored by residence time (flow t = 0.48 s).

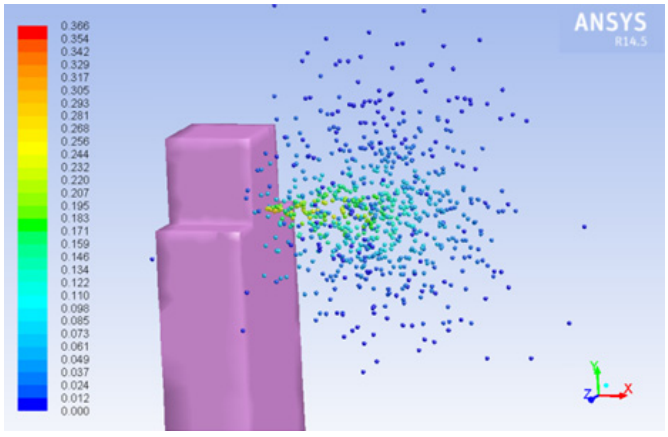

Figure 2-2C Particle velocity (m/s) at flow time = 0.48 s.

Figure 3

Case 1, the shape of the coughing jet at the end of coughing (0.48 s). Particle distribution overlay with velocity contours (top and side views). Particle diameter = 10 µm.

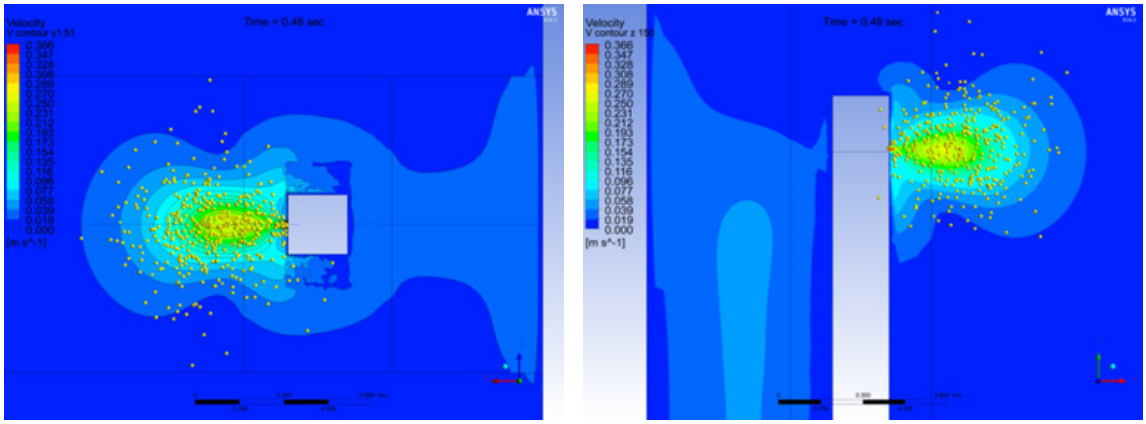

Figure 4

Particle distribution at the end of coughing (0.48 s). (Left) Case 4: Particle diameter = 10 µm. (Right) Case 2: Particle diameter = 5 µm.

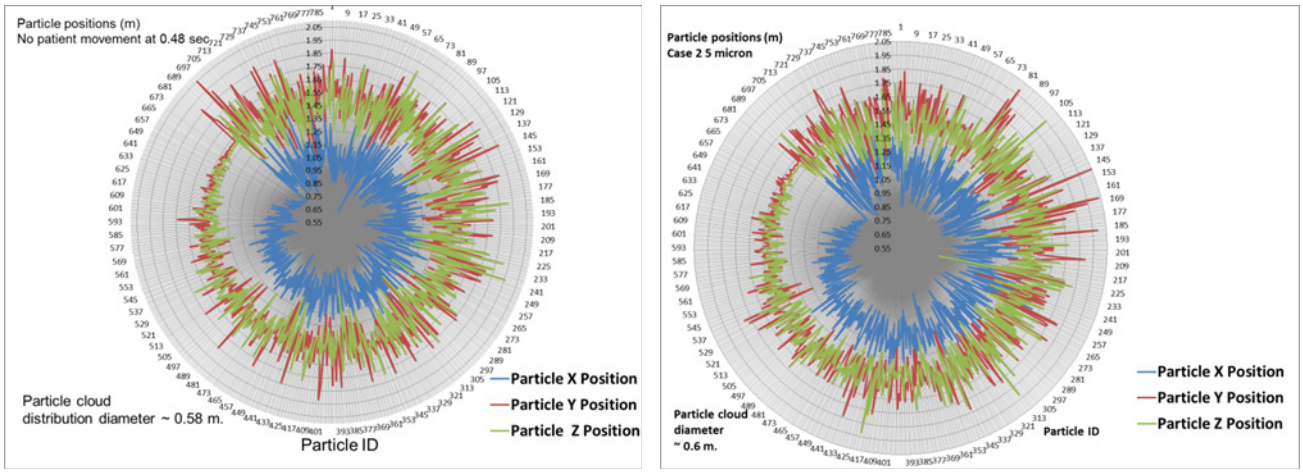

Figure 5

Particle distribution during the initial coughing phase. Case 4: Particle diameter = 10 µm.

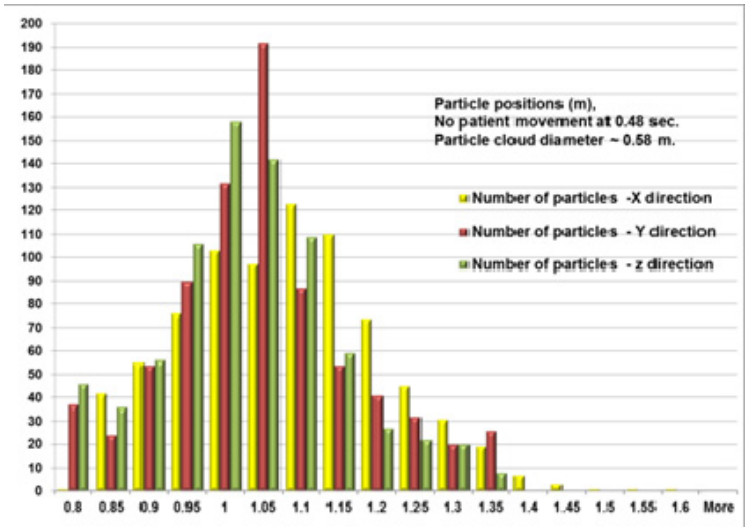

of Figure 2, the particles would stay together if the turbulence dispersion behavior was not considered.

Patient Movement Phase (0.5-3.8 Seconds)

Figure 7 displays the percentage of particles distributed in the upper, breathing, lower, and near-floor zones from 0-400 seconds. The breathing zone curve could be viewed as the contaminant exposure curve. As shown in Figure 8, the 10-µm particles dropped quickly after coughing during the first 10 seconds because of gravity. Similar to the experimental results of Poussou et al. (2010), a series of "top" vortexes and two series of "side" vortexes were observed during walking when the patient passed through the particle cloud (Figure 9): The "top" vortexes were shedded from

Figure 6

Particle dispersion at the end of coughing (0.48 s), without any turbulence dispersion effects. Particle diameter = 10 µm.

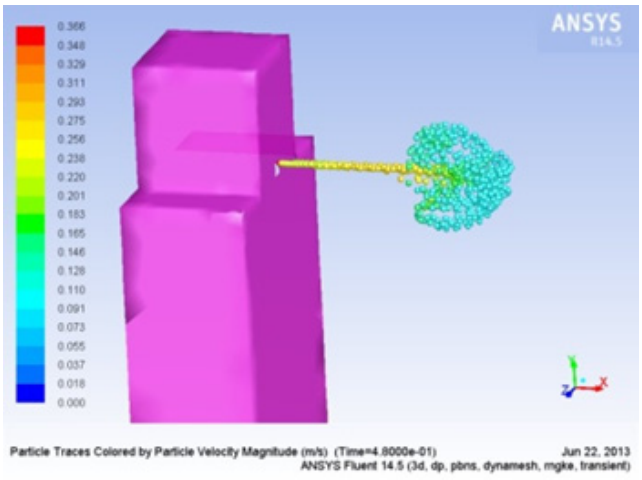

Figure 7

Temporal variations of particle distribution in the upper, breathing, lower, and near-floor zones.

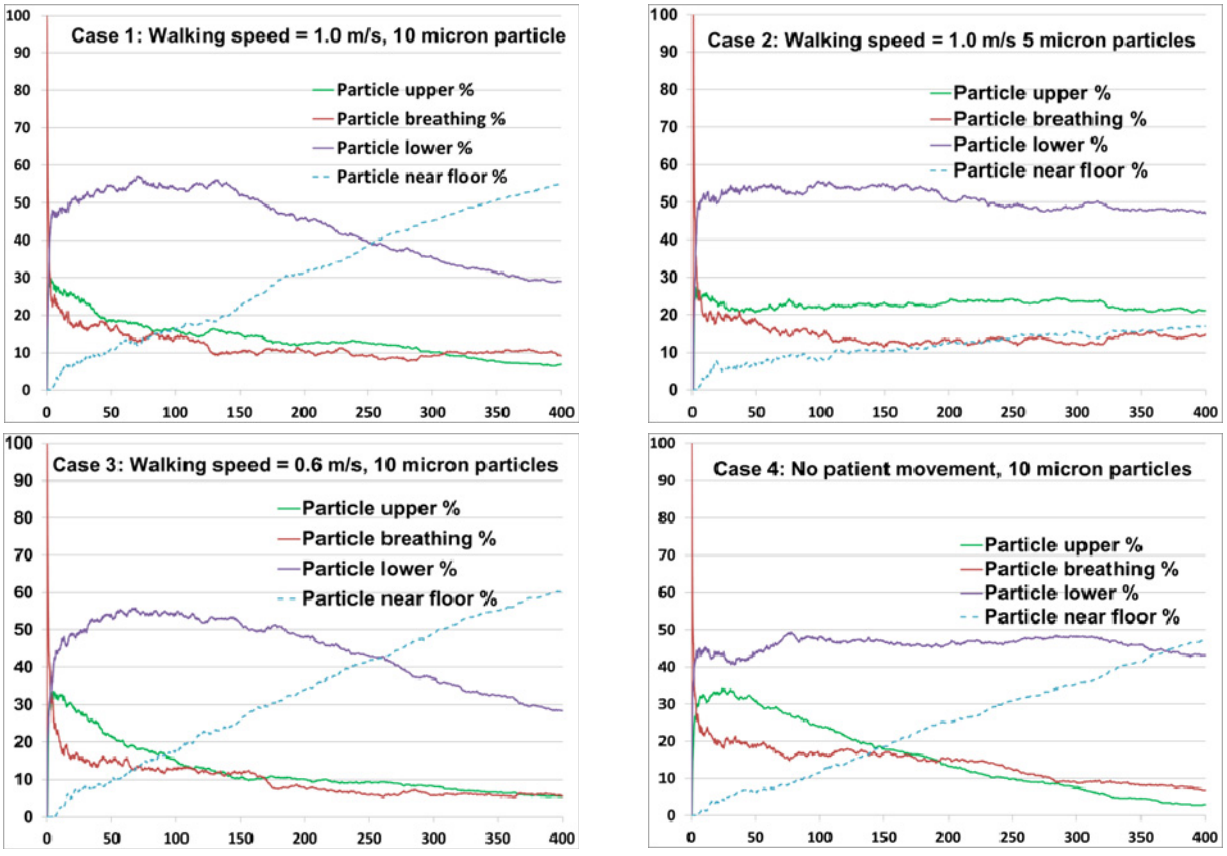

Figure 8

Case 1: Temporal variations of particle distribution in the first 10 s.

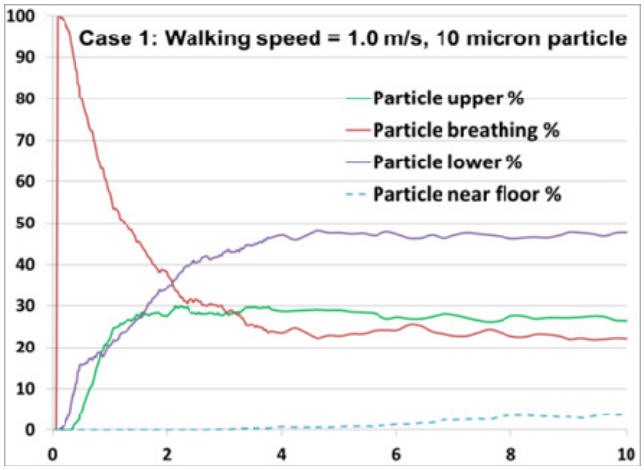

Figure 9

Velocity contour through y = 1.51 m, z = 1.5 m, and the 3-dimensional velocity streamline. Case 1: 2.5 s, walking speed = 1.0 m/s. Max speed = 1.316 m/s.

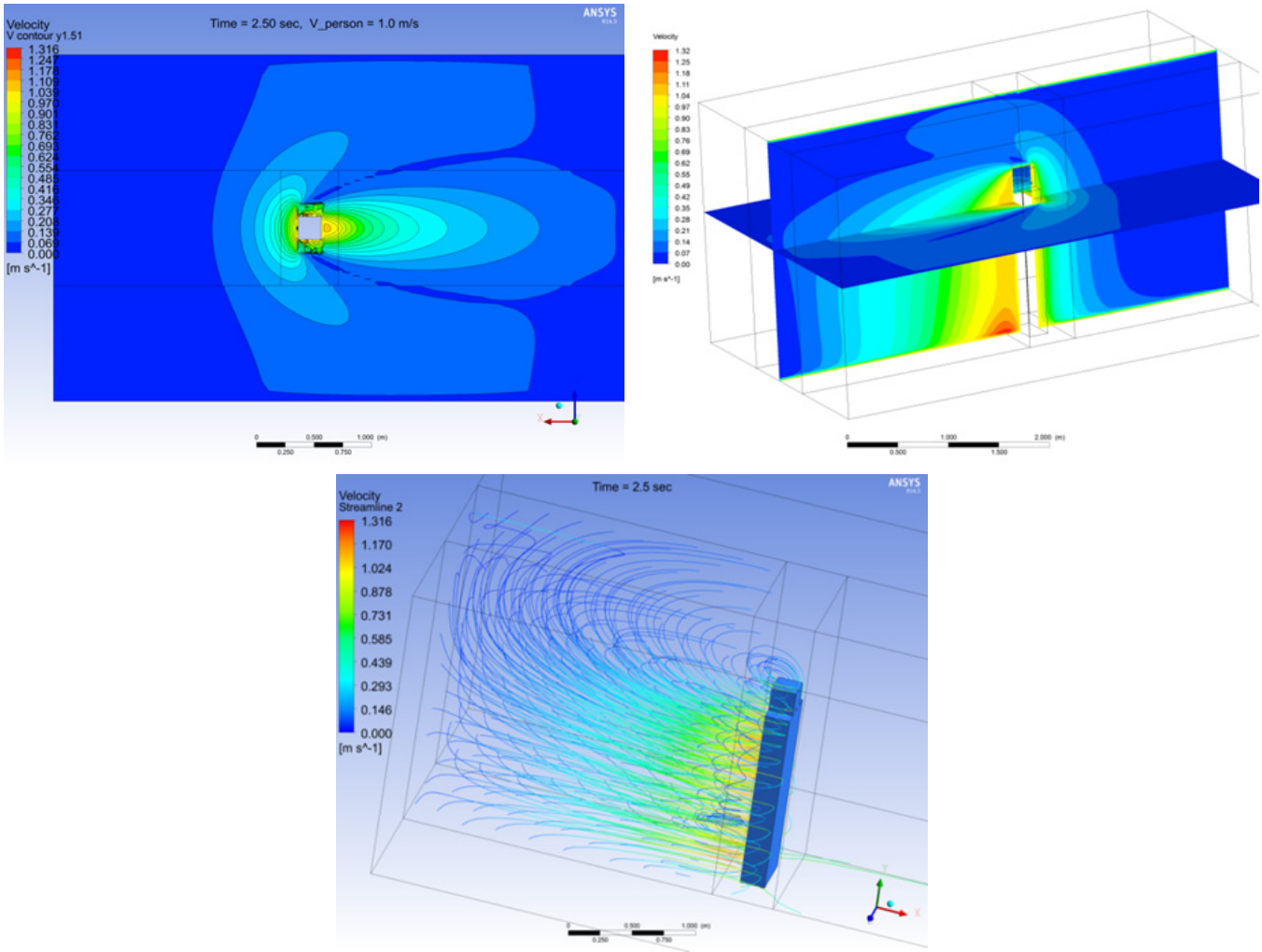

the back of the head to the wake zone (about 1.2 m long when the walking speed was 1 m/s). The top vortexes contributed to the particle upward movement and sent some particles to the space above the patient's head. These particles would stay at the upper and the breathing zones, which could increase the risk of disease transmission through inhalation. Two symmetric side vortexes were alternatively formed from both sides. When they met at the vertical centerline of the moving body, the resultant velocity was larger than the speed velocity. For example, when the walking speed was 1 m/s, the maximum speed at the back of the person was approximately 1.3 m/s in the wake zone (Figure 9). It was also observed that the induced air velocity was higher at the lower level than at the upper level (Figure 10). The amplified air velocity field enhanced the particle entrainment and increased the risk of contaminant in the whole room.

As depicted in Figure 11, when the patient walked through the particle cloud, the particles were entrained into the wake zone by the turbulent flow, and transported along the traveling direction up to approximately 5 m (the full room length) away from the patient by both convective diffusion and turbulence dispersion.

Stationary Flow Phase (3.8-400 Seconds)

Comparing the results from the 5-µm and 10-µm tests, the larger particles deposited more quickly. Small particles tended to suspend in the calm air and the falling rate was very slow (slope of the curve in Figure 7). If the results are extrapolated, it may take more than 700 seconds for most of the 10 µm particles to fall down in a calm indoor environment. As shown in Figure 7, Cases 1 and 4 exhibited very similar particle-falling rates due to the same particle size. Therefore, typical walking speed (0.6 and 1.0 m/s) did not affect the overall particle distribution in the vertical direction at the end of the simulation. The particle size was the dominant factor in terms of the dispersion and deposition.

The air-velocity field in the whole space came to near zero 20-30 seconds after the patient stopped, but the particles were still drifting slowly (<1 cm/s). The stochastic processes, such as turbulence dispersion and gravity, were dominant after the air velocity nearly zeroed.

Figure 12 depicts the particle distribution along the traveling (X), vertical (Y), and lateral (Z) directions at the end of simulation (400 seconds). Movements affected the particle distribution along the travel direction. More particles were distributed in the space near the back of the patient because of the forward-moving air flow entrainment and the inertia of the particles. Little difference was observed between the walking speeds of 1.0 and 0.6 m/s due to the turbulence dispersion. Smaller particles tended to be more evenly distributed along the traveling (X) direction as less particles fell down.

In Case 4, at the end of the simulation, most particles stayed near the starting point as no patient movement was involved, but 18% of the particles managed to travel farther than 2.5 m (half of the room length) from the coughing residual-velocity field and turbulence dispersion.

In the vertical (Y) direction, smaller particles were more prone to evenly distribute in the space than the larger particles, which increased the risk of contamination. At 400 seconds, only 20% of the 5 µm particles spread in the near-floor zone, while the others were evenly distributed in the whole height of the space. However, more than half of the 10 µm particles were in the near-floor zone; 70% were located in the area lower than the breathing zone. Only 15% were in the breathing zone.

In the lateral (Z) direction, particles were evenly distributed in all cases. Slightly lower concentrations were detected in the center of the patient moving zone (near Z = 1.5 m area).

To further quantify the influence of a single patient's movement on the final particle spatial distribution after 400 seconds, the "information entropy" was calculated by the

Figure 10

Velocity distribution through horizontal lines at the center of the room. (Left) Case 1: Walking speed = 1.0 m/s. (Right) Case 3: Walking speed = 0.6 m/s. Particle diameter = 10 µm. Patient location: z = 2.9 (middle of the room, flow pattern fully established).

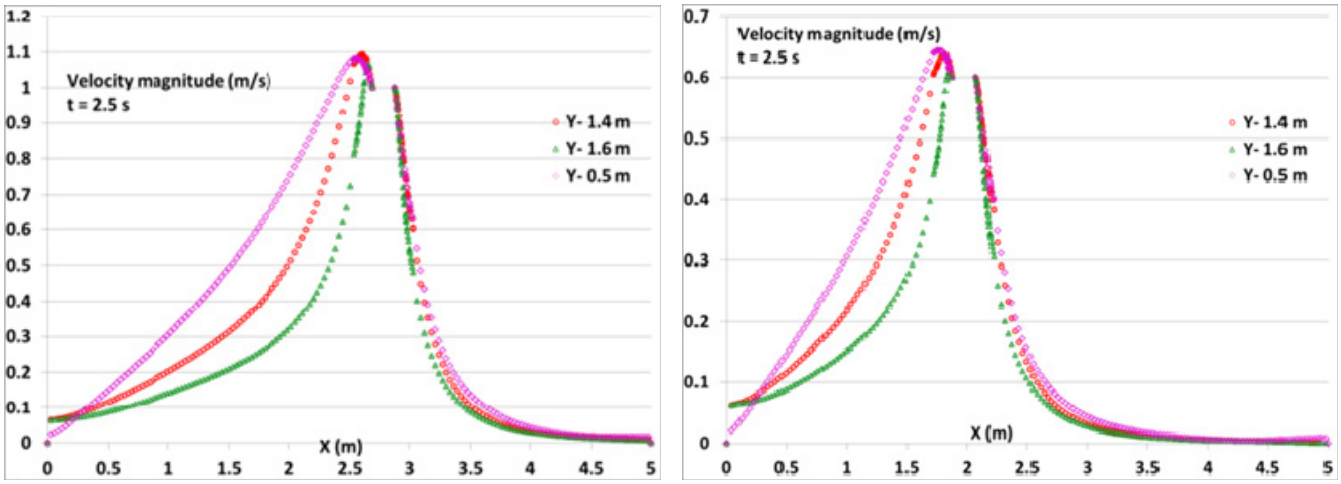

Figure 11

Particle cloud dispersion in the room from 0.5 s to 4.5 s (Case 1: 0.5 s time interval).

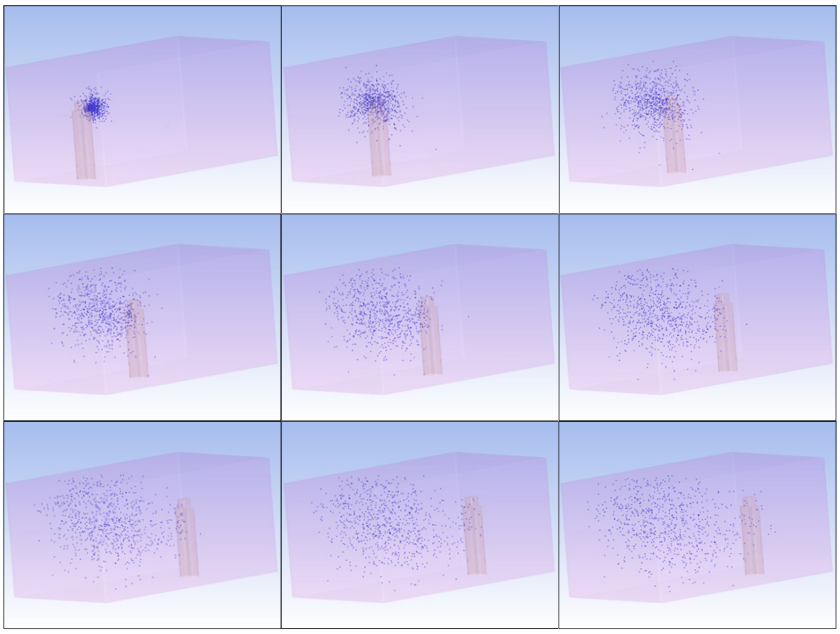

Figure 12

Particle distribution along the movement (X), vertical (Y), and lateral (Z) directions at the end of simulation (400 s). Particle velocity distribution (%) at 400 s.

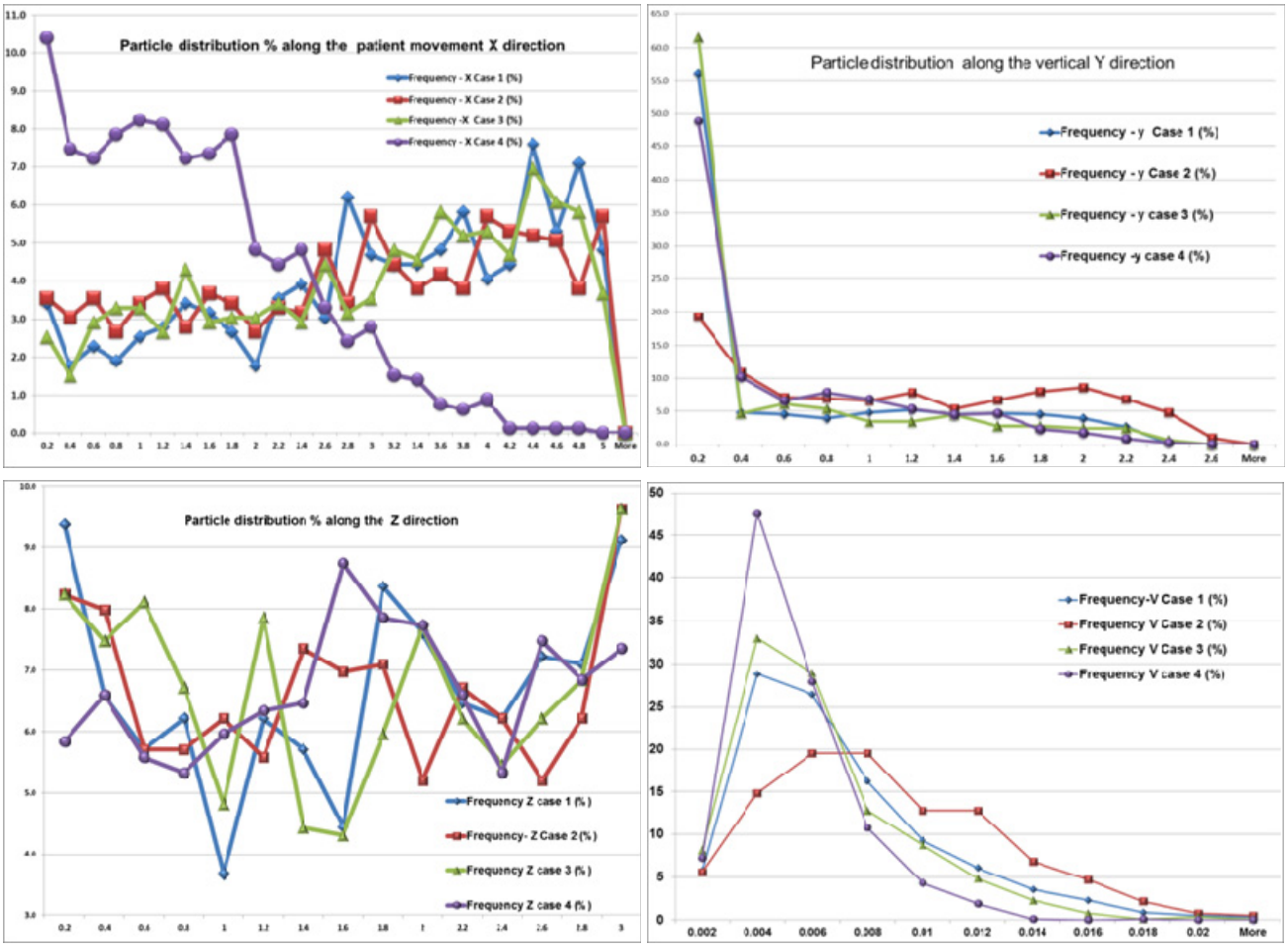

following equation as a measure of disorder in the discrete particle system:

$$H(X) = -\sum_{i=1}^{n} p(x_i) \log p(x_i).$$

where $p(x_i)$ is the probability mass function of outcome x_i. In this study, x_i is the spatial distribution along the traveling (X) direction. Higher entropy implies higher uncertainty (chaotic diffusion) and a higher risk of particle contamination. As shown in Table 3, in the traveling direction, the information entropy of the cases with the patient moving was about 0.5 bit higher than in the case without patient movement. Smaller particles diffused more evenly in the X direction, so the entropy of the 5-µm case was slightly larger than the 10-µm case. The speed of the walking did not affect the entropy as Cases 1 and 3 yielded similar entropy.

At the end of the simulation (400 seconds), the majority of the particles moved in very low velocities (Figure 12). Case 4 exhibited a larger population of lower-speed particles as no patient movement was involved.

To further quantify the importance of turbulence diffusion, Case 5 (without patient movement) was re-run and 10 particle trajectories were sampled. Figure 13 presents the trajectory differentials along the longitudinal (X) direction from the two runs. The standard deviation is ~0.76 m (200-400 seconds) from the two runs of the same case, which is mainly due to the randomness of turbulence diffusion.

Conclusions

Through simulation, this study investigated the interactions between the airflow induced by a patient's movement in a room and the particles discharged by coughing. The following were determined:

1. In the wake zone behind the moving patient, the induced air velocity was higher than the walking speed. The complicated flow structure enhanced the particle entrainment and spread the particles in the whole room.
2. The particle diameter was the controlling factor for particle dispersion and deposition. Small particles tended to suspend in the calm air with an even distribution. The typical patient walking speed had no effect on the falling rates.
3. Walking speed affected the particle distribution in the traveling direction, but not in vertical or lateral directions at the end of the simulation. The risk of particle contamination could be defined by the system entropy or the disorder of spatial particle distribution in the room.
4. The contributions of turbulence dispersion to the particle movement were investigated by examining the particle trajectories. The turbulence dispersion greatly affected the particle movement through the whole process.

Further studies on the initial velocity of a cough, as well as its particle distribution in a well-controlled environment, are needed to provide more accurate CFD boundary conditions.

Table 3

Information entropy of simulated cases along traveling (X) direction.

Case #	Particle Size (µm)	Walking Speed (m/s)	Information Entropy
1 (base)	10	1.0	4.537
2	5	1.0	4.604
3	10	0.6	4.568
4	10	0	4.055

Figure 13

Particle trajectory differentials in the longitudinal (X) direction from two runs of Case 5 (without patient movement).

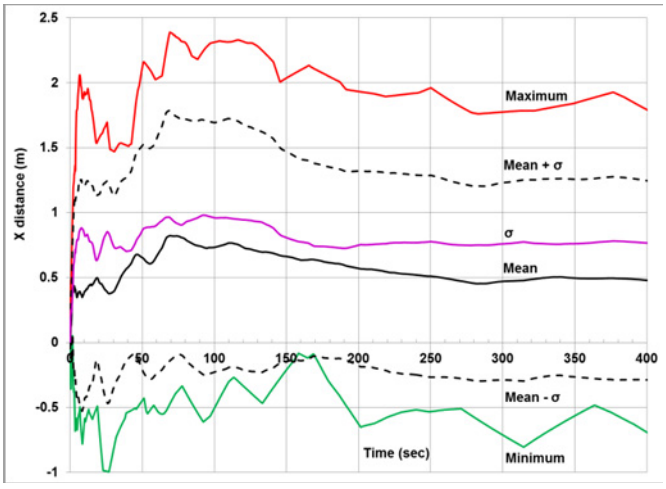

Acknowledgments

*Correspondence should be addressed to Yanzheng (Don) Guan at don.guan@nih.gov.

Disclosure

The authors have nothing to disclose.

References

ANSYS, Inc. ANSYS fluent 14.5 user's guide. Lebanon, NH: ANSYS, Inc.; 2013.

Brohus H, Balling KD, Jeppesen D. Influence of movements on contaminant transport in an operating room. Indoor Air. 2006;16:356-72.

Chao CYH, Wan MP, Morawska L, Johnson GR, Ristovski ZD, Hargreaves M, et al. Characterization of expiration air jets and droplet size distributions immediately at the mouth opening. J Aerosol Sci. 2009;40(2):122-33.

Choi JI, Edwards JR. Large eddy simulation and zonal modeling of human-induced contaminant transport. Indoor Air. 2008;18:233-49.

Choi JI, Edwards JR. Large-eddy simulation of human-induced contaminant transport in room compartments. Indoor Air. 2012;22:77-87.

Duguid JP. The numbers and the sites of origin of the droplets expelled during xpiratory activities. Edinburgh Med J. 1945;52:385-401.

Edwards D, Man J, Brand P, Katstra J, Sommerer K, Stone H, et al. Inhaling to mitigate exhaled bioaerosols. Proc Natl Acad Sci USA. 2004;101(50):17383-8.

Ersahin C. Aerosol generation and entrainment model for cough simulations. Doctoral dissertation, West Virginia University, Morgantown, WV.

Fairchild CI, Stamper JF. Particle concentration in exhaled breath. Am Indus Hyg Assoc J. 1987;48:948-9.

Ge Q, Li X, Inthavong K, Tu J. Numerical study of the effects of human body heat on particle transport and inhalation in indoor environment. Build Environ. 2013;59:1-9.

Gupta JK, Lin CH, Chen Q. Flow dynamics and characterization of a cough. Indoor Air. 2009;19:517-25.

Gupta JK, Lin CH, Chen Q. Inhalation of expiratory droplets in aircraft cabins. Indoor Air. 2011;21(4):341-50.

Hathway E. CFD modelling of pathogen transport due to human activity. Doctoral dissertation, University of Leeds, UK.

Jennison M. Atomizing of mouth and nose secretions into the air as revealed by high speed photography. Aerobiol. 1942;17:106-28.

Johnson GR, Morawskaa L, Ristovskia ZD, Hargreavesa M, Mengersena K, et al. Modality of human expired aerosol size distributions. J Aerosol Sci. 2011;42:839-51.

Kwon S, Park J, Jang J, Cho Y, Park D, Kim C, et al. Study on the initial velocity distribution of exhaled air from coughing and speaking. Chemosphere. 2012;87:1260-4.

Lin H, Zhao B. A numerical study of influence of human body movement on indoor airflow and contaminants distribution. In: Proceedings of HB2012: Int'l Society of Indoor Air Quality and Climate. Santa Cruz, CA: Int'l Society of Indoor Air Quality and Climate; 2012.

Loudon R, Roberts R. Droplet expulsion from the respiratory tract. Am Rev Resp Dis. 1967;95:435-42.

Mazumdar S. Transmission of airborne contaminants in airliner cabins. Doctoral dissertation, Purdue University, West Lafayette, IN.

Mazumdar S, Chen Q. Impact of moving bodies on airflow and contaminant transport inside aircraft cabins. The 10th International Conference on Air Distribution in Rooms. Helsinki, Finland; 2007.

Mazumdar S, Yin Y, Guity A, Marmion P, Gulick B, Chen Q. Impact of moving objects on contaminant concentration distributions in an inpatient room with displacement ventilation. HVAC&R Res. 2010;16(5):545-64.

Memarzadeh F. Health and safety risk assessment methodology to calculate reverse airflow tolerance in a biosafety level 3 (BSL-3) or airborne infection isolation room (AII) environment. Intl J Risk Assess Mgmt. 2010;14(1/2):157-75.

Memarzadeh F, Xu W. Role of air changes per hour (ACH) in possible transmission of airborne infections. Build Simulation. 2012;5(1):15-28.

Morawska L, Johnson G, Ristovski Z, Hargreaves M, Mengersen K, Corbett S, et al. Size distribution and sites of origin of droplets expelled during expiratory activities. J Aerosol Sci. 2009;40(3):256-69.

Papineni R, Rosenthal FS. The size distribution of droplets in the exhaled breath of healthy human subjects. J Aerosol Med. 1997;10(2):105-16.

Poussou SB, Mazumdar S, Plesniak MW, Sojka PE, Chen Q. Flow and contaminant transport in an airliner cabin induced by a moving body: model experiments and CFD prediction. Atmos Environ. 2010;44(24):2830-9.

Sun W, Ji J. Transport of droplets expelled by coughing in ventilated rooms. Indoor Built Environ. 2007;16:493-504.

Tang JW, Li Y, Eames I, Chan PK, Ridgway GL. Factors involved in the aerosol transmission of infection and control of ventilation in healthcare premises. J Hosp Infect. 2006;64(2):100-14.

Yang S, Lee GWM, Chen CM, Wu CC, Yu KP. The size and concentration of droplets generated by coughing in human subjects. J Aerosol Med. 2007;20(4):484-94.

VanSciver M, Miller S, Hertzberg J. Particle image velocimetry of human cough. Aerosol Sci Technol. 2011;45(3):415-22.

Wang J, Chow T. Numerical investigation of influence of human walking on dispersion and deposition of expiratory droplets in airborne infection isolation room. Build Environ. 2011;46:1993-2002.

Zhai Z, Chen Q, Scanlon PW. Design of ventilation system for an indoor auto racing complex. ASHRAE Transactions. 2002;108(1):989-98.

Zhang L, Li Y. Dispersion of coughed droplets in a fully-occupied high-speed rail cabin. Build Environ. 2012;47:58-66.

Zhu S, Kato S, Yang JH. Study on transport characteristics of saliva droplets produced by coughing in a calm indoor environment. Building Environ. 2006;41(12):1691-702.